Domino-Tiling of Orthogonal Polygon Phased Arrays: An Exhaustive Search Approach

P. Rocca, N. Anselmi, A. Polo, and A. Massa

Contents

1 Introduction

This work presents an innovative tiling optimization strategy for arbitrary orthogonal-polygon shaped apertures. An exhaustive search approach, together with a multi-objective strategy, has been used in order to obtain optimal tiling configurations, jointly optimizing two different pattern features of interest. A simple example validating the proposed method has been finally reported.

2 Numerical Results

2.1 Orthogonal Polygon #7 (Hexagon Small)

Array Analysis Parameters:

- Total Number of Elements: $P = 48$
- Spacing: $d = \lambda/2$
- Number of Samples along u: 256
- Number of Samples along v: 256
- Steering θ Direction: $\theta_s = 0$
- Steering ϕ Direction: $\phi_s = 0$

Tiling Parameters:

- Number of Inner Lattice Points: $N_{inn} = 33$
- Number of Outer Lattice Points: $N_{out} = 33$
- Number of boundary points $N = 33$
- Number of cells $N_{cel} = 48$
- Number of tiling Configurations: $T = 39028$

2.1.1 ETM-MOP - CP Reference Excitations, Symmetric Mask - Mask Matching vs {SLL, D, HPBW} , SLL vs {D, HPBW}

Reference Fully-Populated Array:

- Number of Samples along u: 512 $-2 < u < 2$
- Number of Samples along v: 512 $-2 < v < 2$
- Steering θ Direction: $\theta_s = 0$
- Steering ϕ Direction: $\phi_s = 0$
- Tapering: CP Symmetric Mask
- Side lobe level: $SLL = -20.6[dB]$
- Main Lobe Window Width along u: $MW_u = 0.28$ [u]
- Main Lobe Window Width along v: $MW_v = 0.28$ [v]

Synthesis Mask Representation:

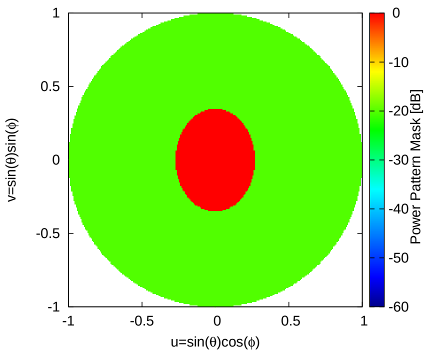

Cost Function:

- $OBJ^{(1)} = D$
- $OBJ^{(2)} = HPBW_{AZ}$
- $OBJ^{(3)} = HPBW_{EL}$
- $OBJ^{(4)} = SLL$
- $OBJ^{(5)} = \int_{-1}^{1}\int_{-1}^{1}\left[M\left(u,v\right)-P\left(u,v;\underline{C}\right)\right]\mathcal{H}\left[P\left(u,v;\underline{C}\right)-M\left(u,v\right)\right]dudv$

Results

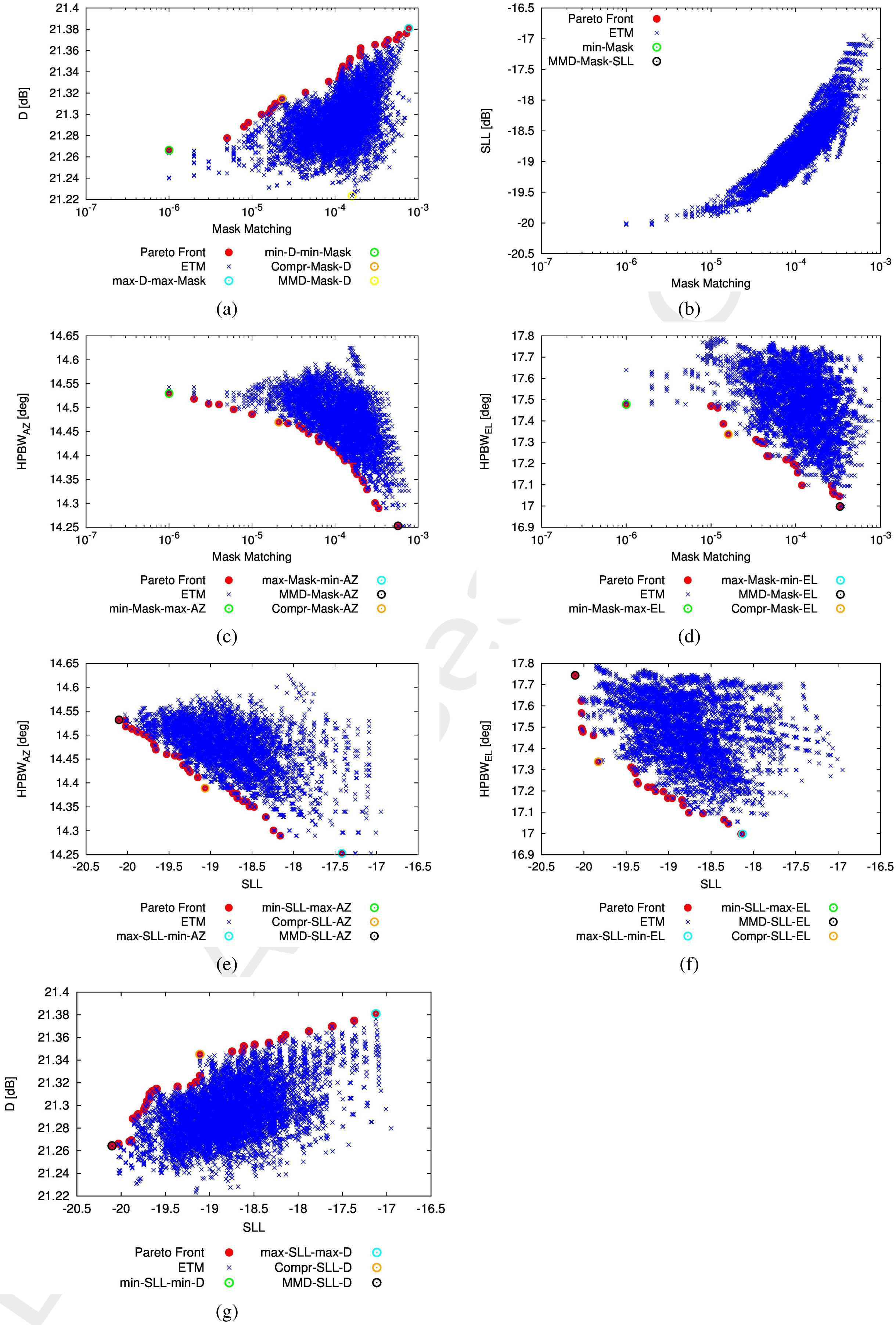

Figure 1: Pareto front of the ETM solutions.

	$Solution\,ID$	SLL [dB]	D [dBi]	$HPBW_{az}$ [deg]	$HPBW_{el}$ [deg]	$Mask\,Matching$
$min - Mask - D$	28240	-20.03	21.27	14.54	17.64	9.99×10^{-7}
$max - D - max - Mask$	21292	-17.12	21.38	14.33	17.47	7.73×10^{-4}
$MMD - mask - D$	14026	-19.16	21.22	14.53	17.20	1.60×10^{-4}
$Compr - mask - D$	15108	-19.60	21.31	14.55	17.67	2.30×10^{-5}
$min - mask - max - AZ$	33723	-20.01	21.24	14.53	17.48	9.99×10^{-7}
$max - mask - min - AZ$	27997	-17.42	21.32	14.25	17.70	5.74×10^{-4}
$Compr - mask - AZ$	18059	-19.66	21.29	14.47	17.70	2.10×10^{-5}
$MMD - mask - AZ$	27997	-17.42	21.32	14.25	17.70	5.74×10^{-4}
$min - mask - max - EL$	33723	-20.01	21.24	14.53	17.48	9.99×10^{-7}
$max - mask - min - EL$	13627	-18.13	21.28	14.53	17.00	3.32×10^{-4}
$MMD - Mask - EL$	13627	-18.13	21.28	14.53	17.00	3.32×10^{-4}
$Compr - Mask - EL$	14027	-19.83	21.23	14.53	17.34	1.60×10^{-5}
$min - Mask - SLL$	39027	-20.10	21.26	14.53	17.74	0
$MMD - Mask - SLL$	39027	-20.10	21.26	14.53	17.74	0
$min - D - min - SLL$	39027	-20.10	21.26	14.53	17.74	0
$max - SLL - max - D$	21292	-17.12	21.38	14.33	17.47	7.73×10^{-4}
$Compr - SLL - D$	15009	-19.11	21.35	14.54	17.62	1.24×10^{-4}
$MMD - SLL - D$	39027	-20.10	21.26	14.53	17.74	0
$max - SLL - min - AZ$	27997	-17.42	21.32	14.25	17.70	5.74×10^{-4}
$min - SLL - max - AZ$	39027	-20.10	21.26	14.53	17.74	0
$Compr - SLL - AZ$	18106	-19.07	21.30	14.39	17.67	1.33×10^{-4}
$MMD - SLL - AZ$	39027	-20.10	21.26	14.53	17.74	0
$max - SLL - min - EL$	13627	-18.13	21.28	14.53	17.00	3.32×10^{-4}
$min - SLL - max - EL$	39027	-20.10	21.26	14.53	17.74	0
$MMD - SLL - EL$	39027	-20.10	21.26	14.53	17.74	0
$Compr - SLL - EL$	14027	-19.83	21.23	14.53	17.34	1.60×10^{-5}

Table I: Pattern descriptors for the presented solutions.

Observations:

In plot (b), due to the mask matching value of the solution $ID = 39027$, this value are not representable in the plot. However, in other plots that don't consider mask matching values (e.g. (e)(f)(g)), the solution $ID = 39027$ is correctly represented.

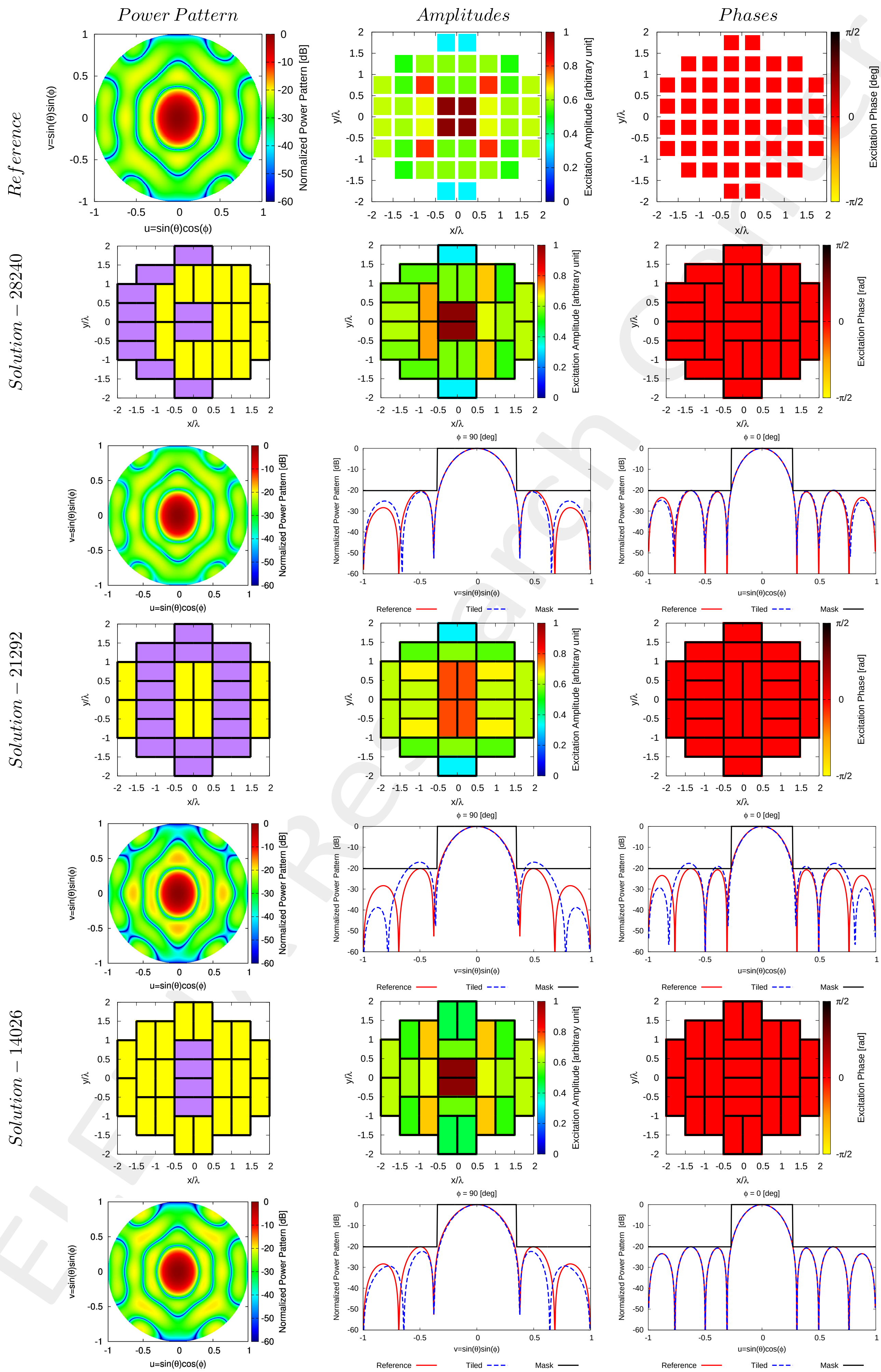

Figure 2: Tiling solutions 1-3.

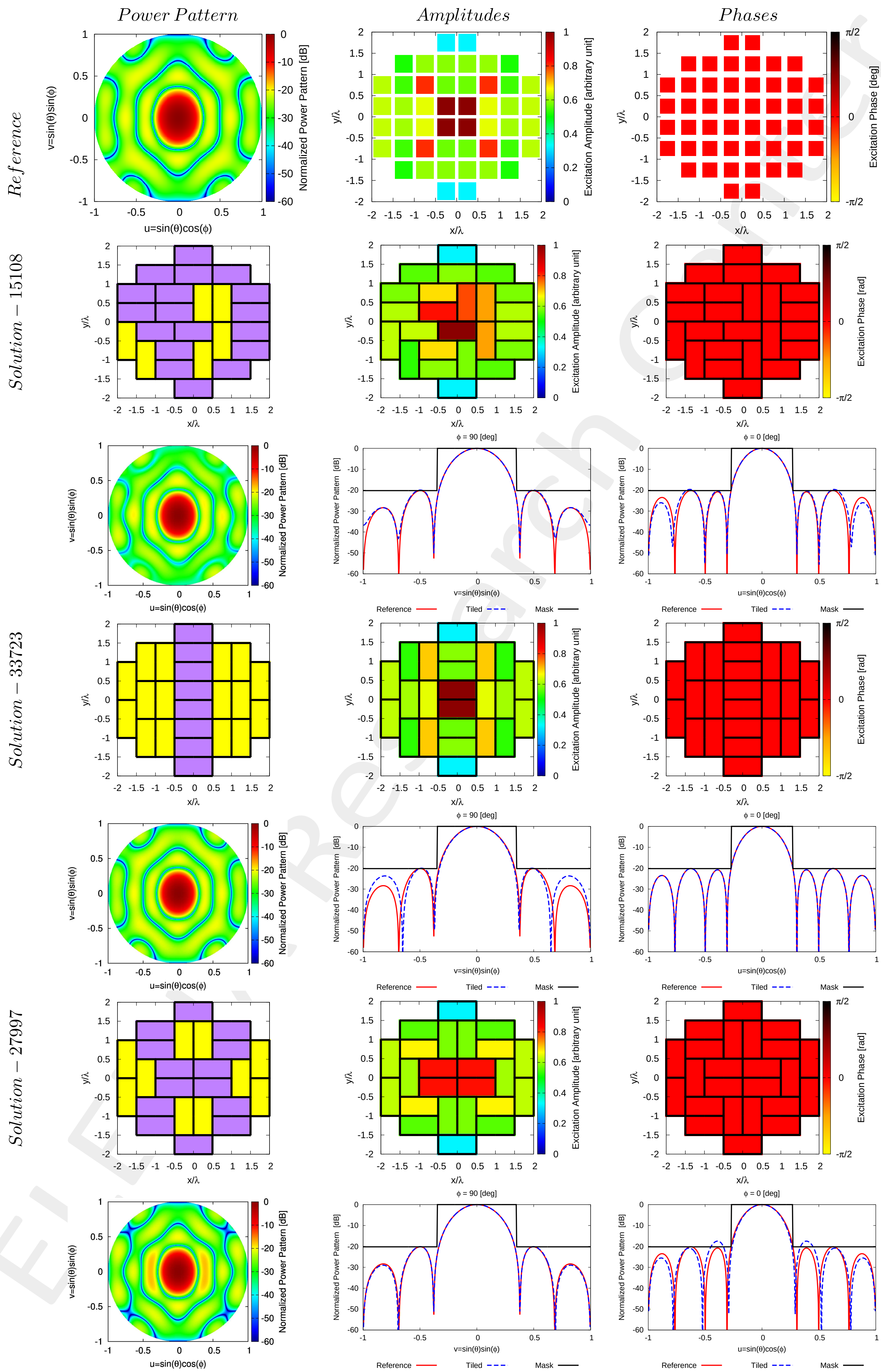

Figure 3: Tiling solutions 4-6.

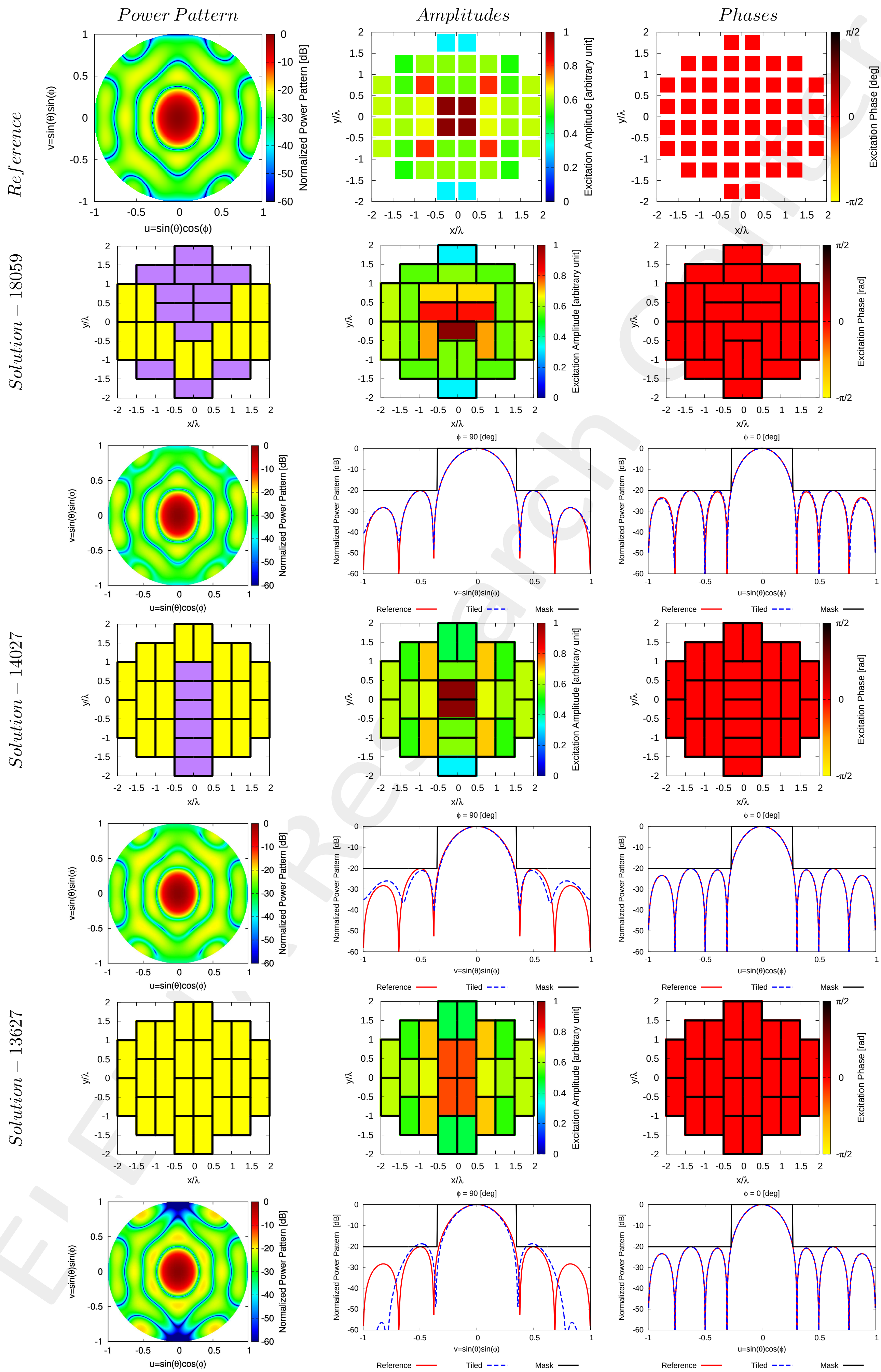

Figure 4: Tiling solutions 7-9.

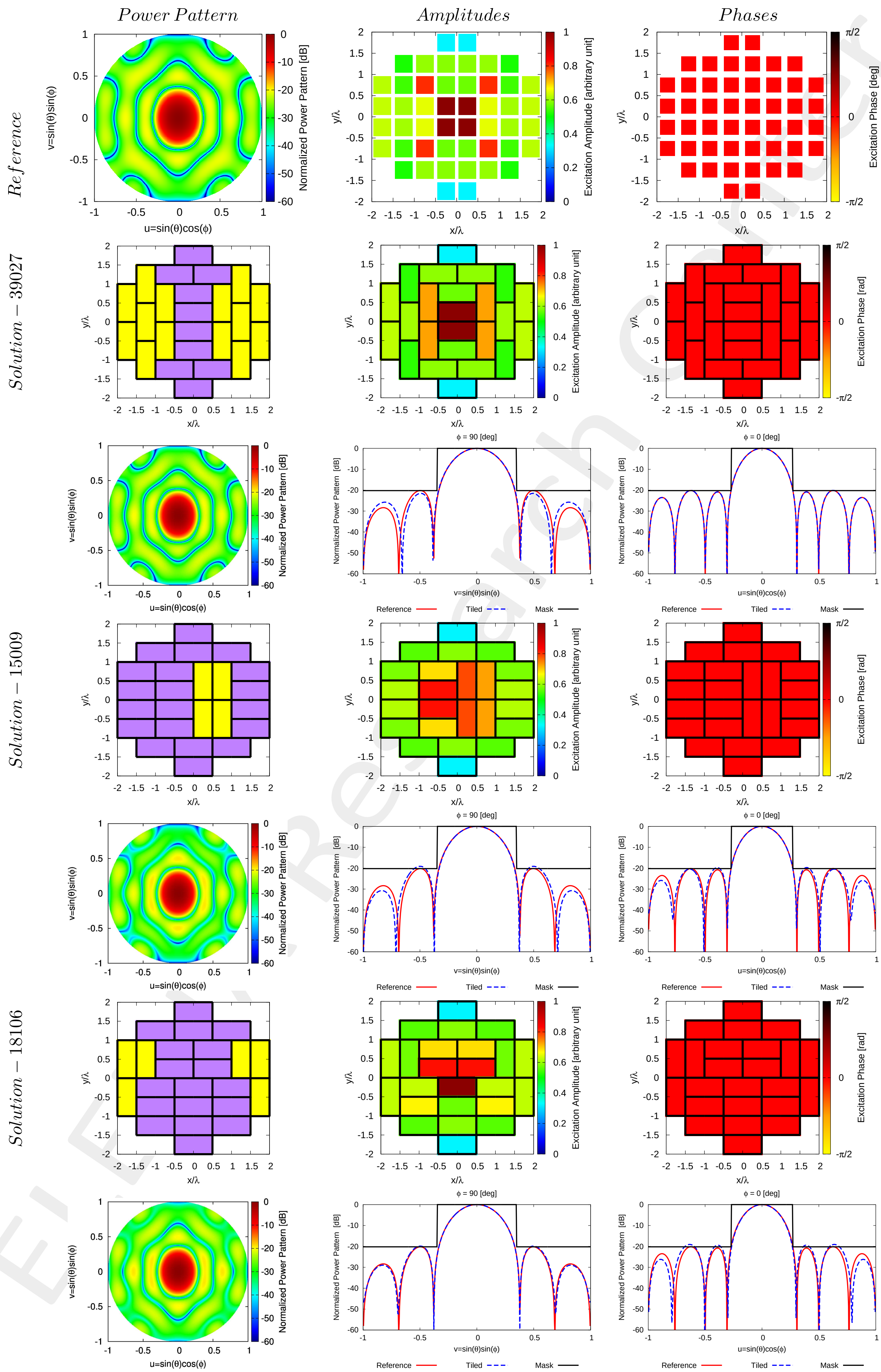

Figure 5: Tiling solutions 10-12.

Observations:

- The twelve solutions are chosen among all pareto solutions, considering different criteria: the solution that minimise the first objective, the solution that minimise the second objective, the solution given by Minimum Manhattan distance and a solution that represent a good compromise between objectives.
- In the plot (a) the MMD represent a poor result due to low levels of mask matching and directivity.
- In the plot (b) all the solutions are overlapped each others.
- In plots (c)(d) the MMD is overlapped with the solution that minimise the $HPBW$.
- In plots (e)(f) the MMD is overlapped with the solution that maximise the $HPBW$.
- In the plot (g) the MMD is overlapped with the solution that minimise SLL and D.

When a black circle is present there will be an overlap between different solutions, so one is hided from the other. Some solutions are present in more plots, so in the table, every ID is associated to the value that minimise or represent.

2.1.2 ETM-MOP - CP Reference Excitations, Asymmetric Mask - Mask Matching vs {SLL, D, HPBW} , SLL vs {D, HPBW}

Reference Fully-Populated Array:

- Number of Samples along u: 512 $-2 < u < 2$
- Number of Samples along v: 512 $-2 < v < 2$
- Steering θ Direction: $\theta_s = 0$
- Steering ϕ Direction: $\phi_s = 0$
- Tapering: CP Asymmetric Mask
- Side lobe level: $SLL = -20.6[dB]$
- Main Lobe Window Width along u: $MW_u = 0.28$ [u]
- Main Lobe Window Width along v: $MW_v = 0.28$ [v]

Synthesis Mask Representation:

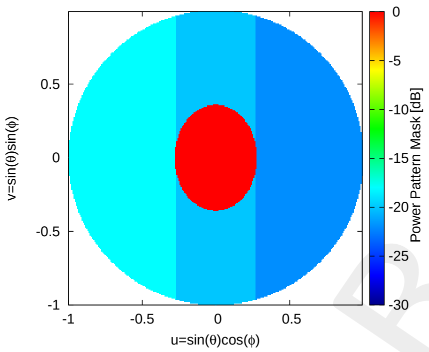

Cost Function:

- $OBJ^{(1)} = D$
- $OBJ^{(2)} = HPBW_{AZ}$
- $OBJ^{(3)} = HPBW_{EL}$
- $OBJ^{(4)} = SLL$
- $OBJ^{(5)} = \int_{-1}^{1}\int_{-1}^{1}\left[M\left(u,v\right) - P\left(u,v;\underline{C}\right)\right]\mathcal{H}\left[P\left(u,v;\underline{C}\right) - M\left(u,v\right)\right]dudv$

Results

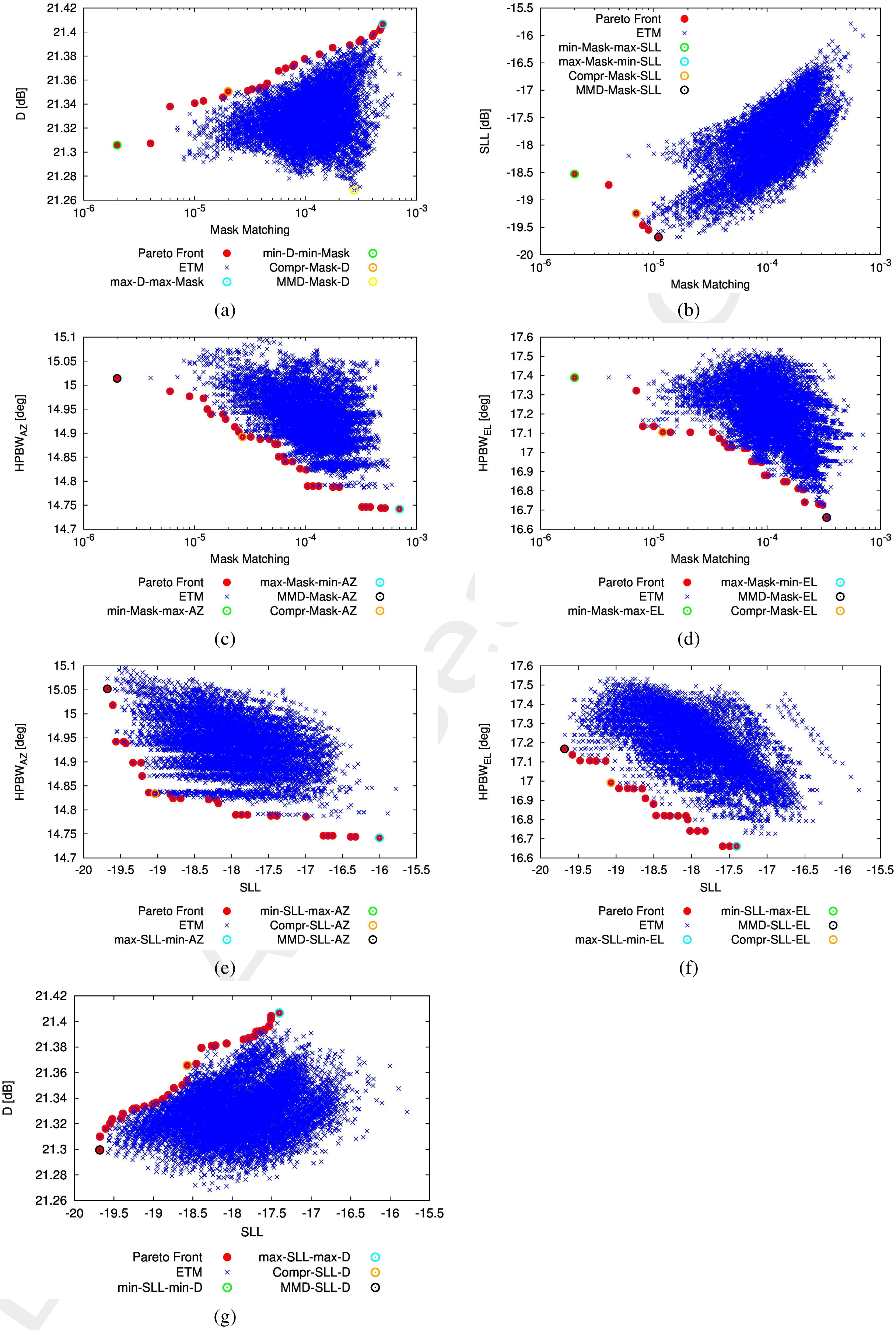

Figure 6: Pareto front of the ETM solutions.

	$Solution\,ID$	SLL [dB]	D [dBi]	$HPBW_{az}$ [deg]	$HPBW_{el}$ [deg]	$Mask\,Matching$
$min-Mask-D$	39028	-18.53	21.31	15.01	17.39	2.00×10^{-6}
$max-D-max-Mask$	21441	-17.40	21.41	14.83	17.22	4.95×10^{-4}
$MMD-mask-D$	13879	-18.29	21.27	15.05	16.82	2.74×10^{-4}
$Compr-mask-D$	29646	-18.26	21.35	14.98	17.37	2.00×10^{-5}
$min-mask-max-AZ$	39028	-18.53	21.31	15.01	17.39	2.00×10^{-6}
$max-mask-min-AZ$	8491	-16.00	21.37	14.74	17.09	7.00×10^{-4}
$Compr-mask-AZ$	28375	-18.47	21.32	14.89	17.35	2.70×10^{-5}
$MMD-mask-AZ$	8491	-16.00	21.37	14.74	17.09	7.00×10^{-4}
$min-mask-max-EL$	39028	-18.53	21.31	15.01	17.39	2.00×10^{-6}
$max-mask-min-EL$	13627	-17.40	21.31	15.04	16.66	3.35×10^{-4}
$MMD-Mask-EL$	13627	-17.40	21.31	15.04	16.66	3.35×10^{-4}
$Compr-Mask-EL$	33576	-19.26	21.30	15.05	17.10	1.20×10^{-5}
$max-Mask-min-SLL$	35236	-19.68	21.30	15.05	17.17	1.10×10^{-5}
$max-SLL-min-Mask$	39028	-18.53	21.31	15.01	17.39	2.00×10^{-6}
$MMD-Mask-SLL$	35236	-19.68	21.30	15.05	17.17	1.10×10^{-5}
$Compr-Mask-SLL$	35178	-19.25	21.32	15.02	17.32	7.00×10^{-6}
$min-D-min-SLL$	35236	-19.68	21.30	15.05	17.17	1.10×10^{-5}
$max-SLL-max-D$	21441	-17.40	21.41	14.83	17.22	4.95×10^{-4}
$Compr-SLL-D$	15140	-18.57	21.37	15.00	17.31	1.40×10^{-4}
$MMD-SLL-D$	35236	-19.68	21.30	15.05	17.17	1.10×10^{-5}
$max-SLL-min-AZ$	8491	-16.00	21.37	14.74	17.09	7.00×10^{-4}
$min-SLL-max-AZ$	35236	-19.68	21.30	15.05	17.17	1.10×10^{-5}
$Compr-SLL-AZ$	25258	-19.04	21.31	14.83	17.53	1.28×10^{-4}
$MMD-SLL-AZ$	35236	-19.68	21.30	15.05	17.17	1.10×10^{-5}
$max-SLL-min-EL$	13627	-17.40	21.31	15.04	16.66	3.35×10^{-4}
$min-SLL-max-EL$	35236	-19.68	21.30	15.05	17.17	1.10×10^{-5}
$MMD-SLL-EL$	35236	-19.68	21.30	15.05	17.17	1.10×10^{-5}
$Compr-SLL-EL$	35233	-19.07	21.29	15.05	17.00	8.00×10^{-5}

Table II: Pattern descriptors for the presented solutions.

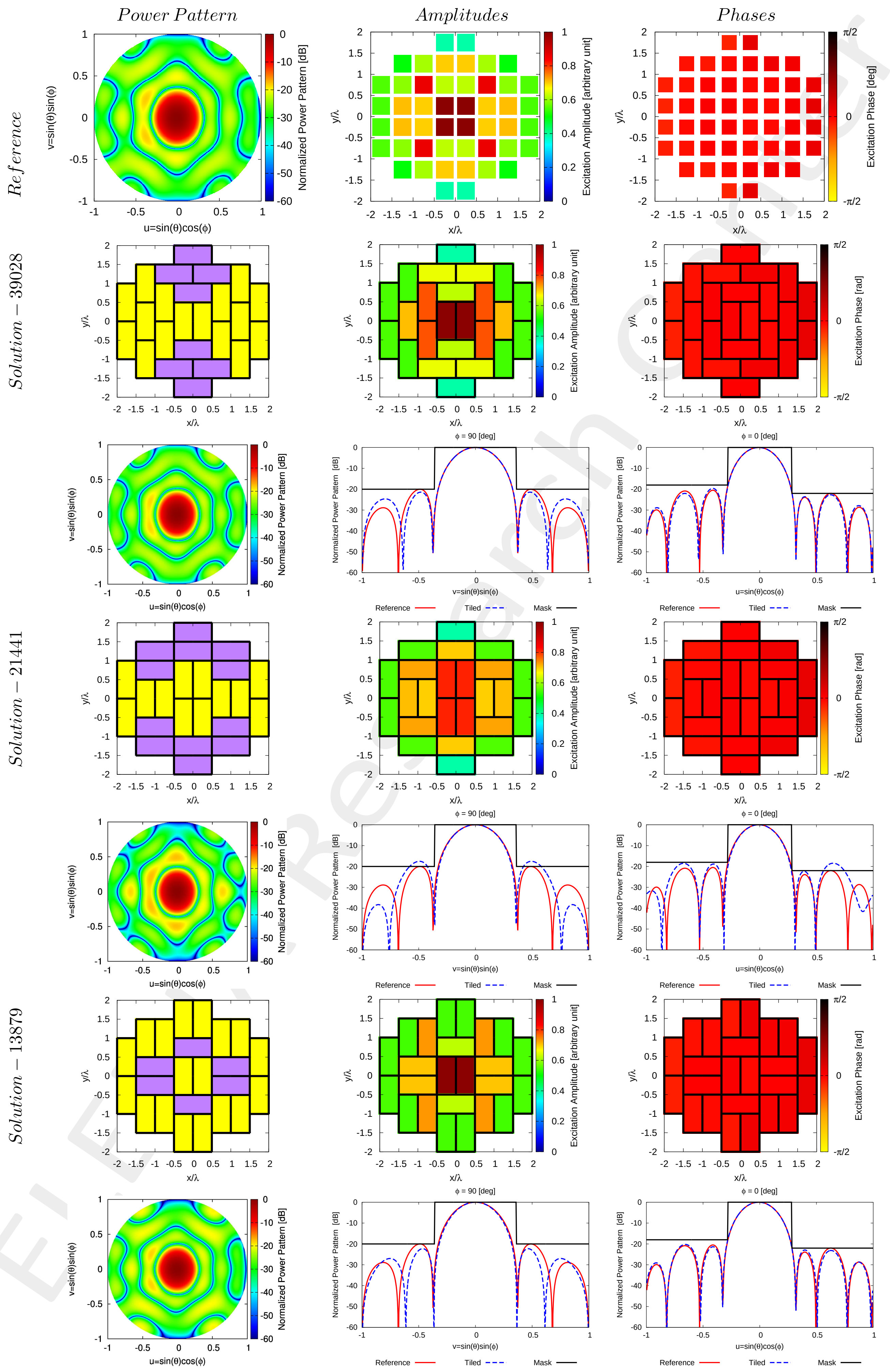

Figure 7: Tiling solutions 1-3.

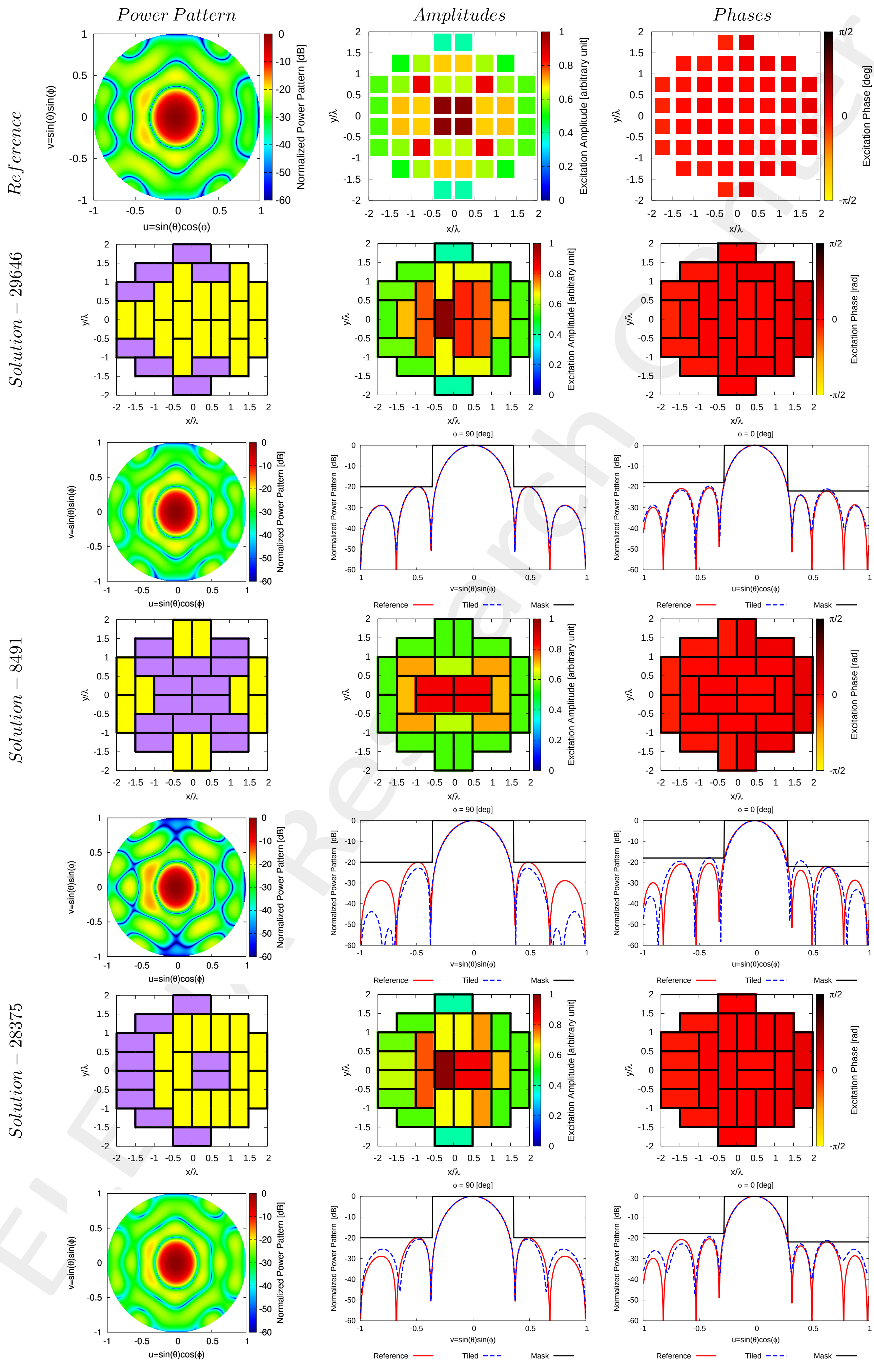

Figure 8: Tiling solutions 4-6.

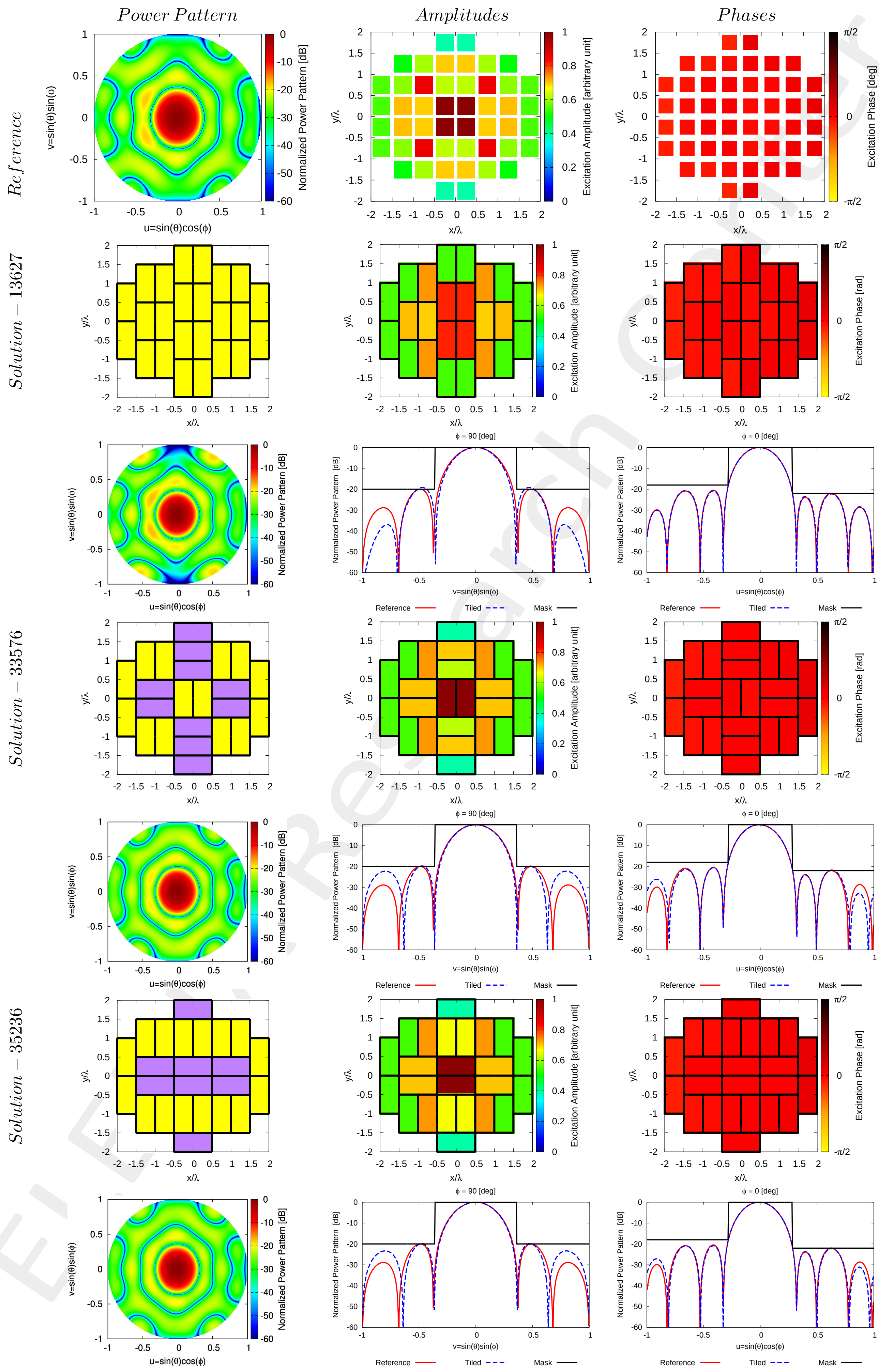

Figure 9: Tiling solutions 7-9.

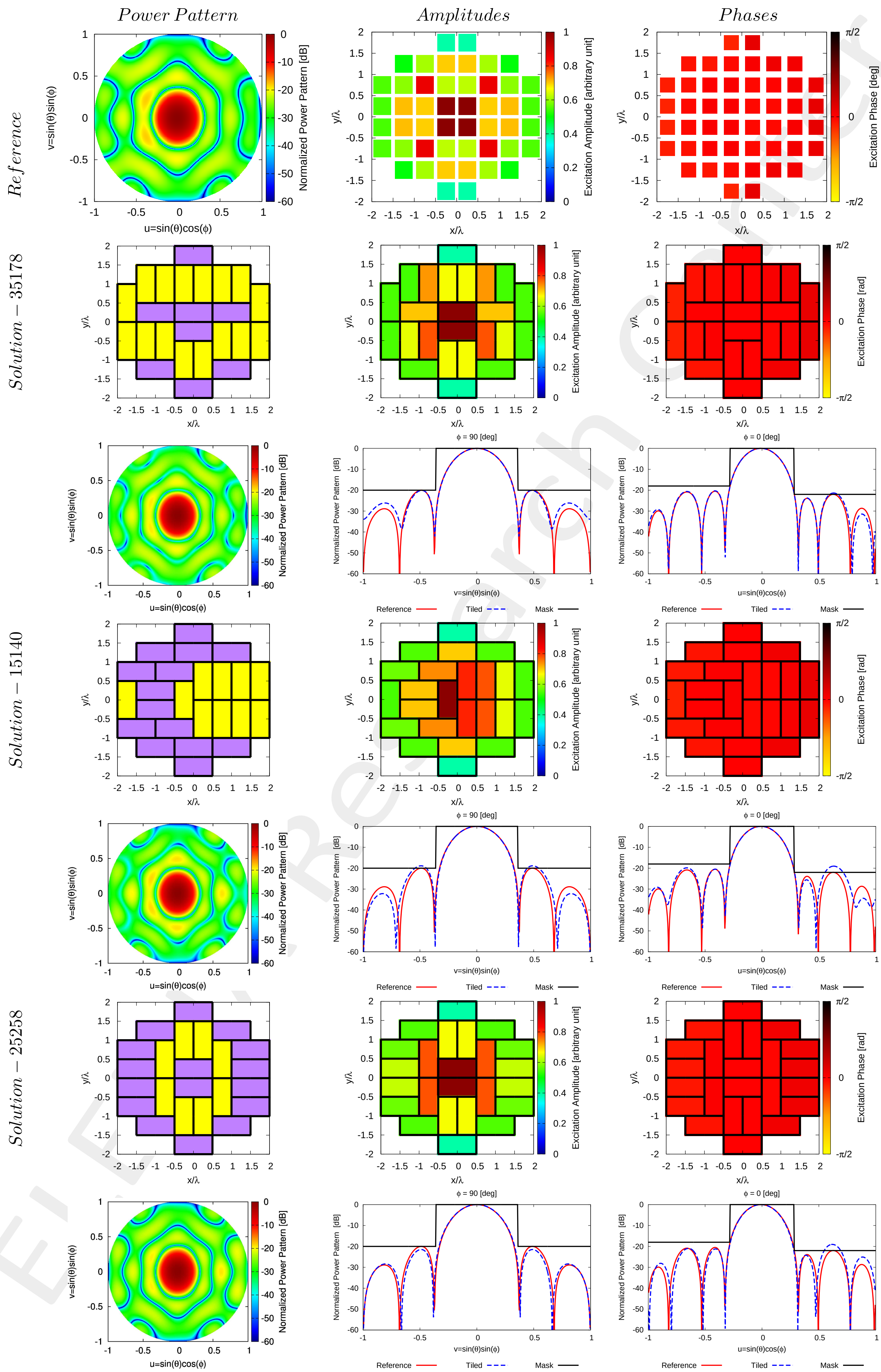

Figure 10: Tiling solutions 10-12.

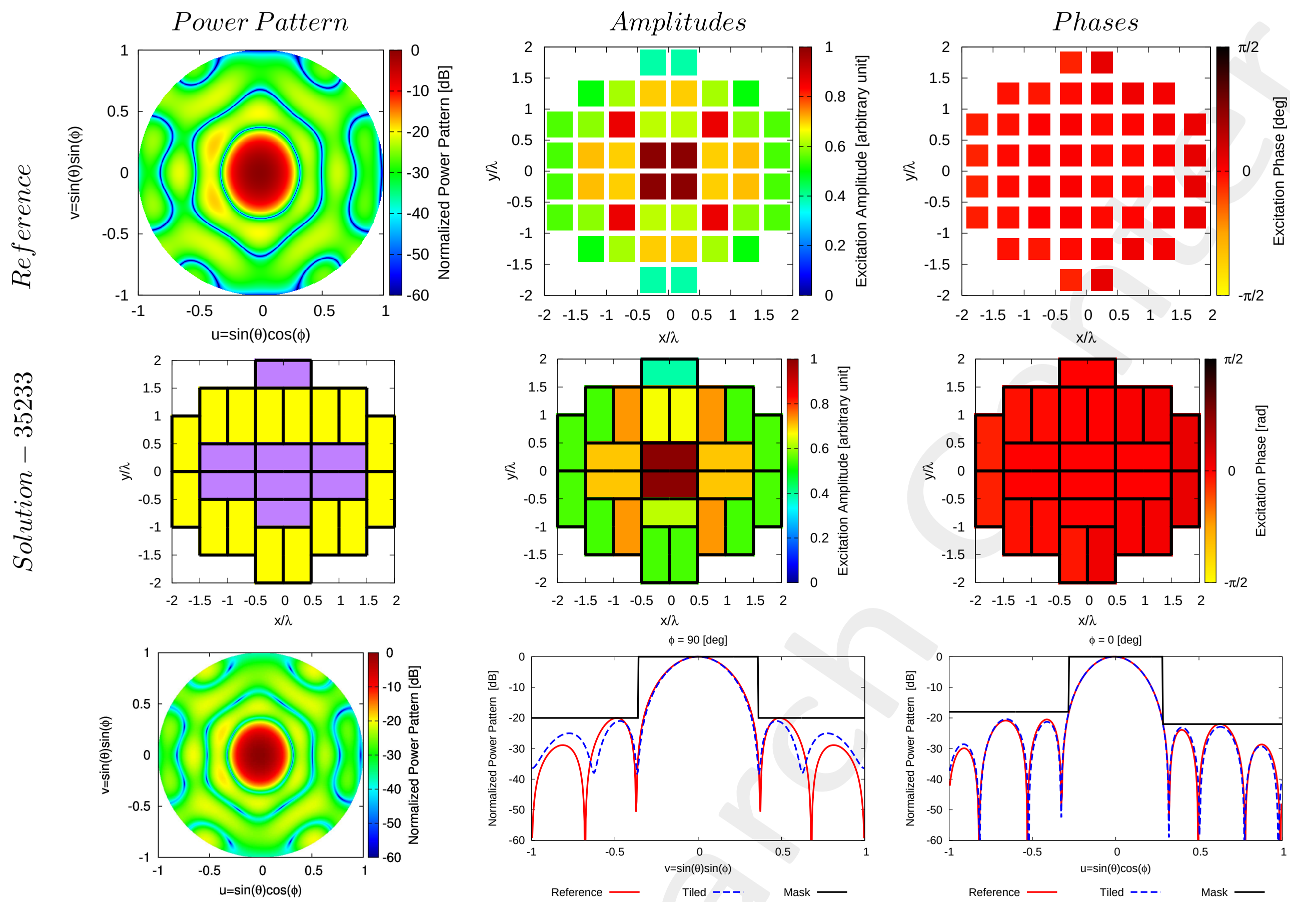

Figure 11: Tiling solutions 13.

Observations:

- The twelve solutions are chosen among all pareto solutions, considering different criteria: the solution that minimise the first objective, the solution that minimise the second objective, the solution given by Minimum Manhattan distance and a solution that represent a good compromise between objectives.
- In the plot (a) the MMD represent a poor result due to low levels of mask matching and directivity.
- In the plot (b) the MMD is overlapped with the solution that minimise the SLL.
- In the plot (c) the MMD is overlapped with the solution that maximise the $HPBW$.
- In the plot (d) the MMD is overlapped with the solution that minimise the $HPBW$.
- In plots (e)(f) the MMD is overlapped with the solution that maximise the $HPBW$.
- In the plot (g) the MMD is overlapped with the solution that minimise SLL and D.

When a black circle is present there will be an overlap between different solutions, so one is hided from the other. Some solutions are present in more plots, so in the table, every ID is associated to the value that minimise or represent.

More information on the topics of this document can be found in the following list of references.

References

[1] M. Salucci, G. Gottardi, N. Anselmi, and G. Oliveri, "Planar thinned array design by hybrid analytical-stochastic optimization," IET Microwaves, Antennas & Propagation, vol. 11, no. 13, pp. 1841-1845, Oct. 2017

[2] P. Rocca, N. Anselmi, A. Polo, and A. Massa, "Pareto-optimal domino-tiling of orthogonal polygon phased arrays," IEEE Trans. Antennas Propag., vol. 70, no. 5, pp. 3329-3342, May 2022.

[3] P. Rocca, N. Anselmi, A. Polo, and A. Massa, "An irregular two-sizes square tiling method for the design of isophoric phased arrays," IEEE Trans. Antennas Propag., vol. 68, no. 6, pp. 4437-4449, Jun. 2020.

[4] P. Rocca, N. Anselmi, A. Polo, and A. Massa, "Modular design of hexagonal phased arrays through diamond tiles," IEEE Trans. Antennas Propag., vol.68, no. 5, pp. 3598-3612, May 2020.

[5] N. Anselmi, L. Poli, P. Rocca, and A. Massa, "Design of simplified array layouts for preliminary experimental testing and validation of large AESAs," IEEE Trans. Antennas Propag., vol. 66, no. 12, pp. 6906-6920, Dec. 2018.

[6] N. Anselmi, P. Rocca, M. Salucci, and A. Massa, "Contiguous phase-clustering in multibeam-on-receive scanning arrays" IEEE Trans. Antennas Propag., vol. 66, no. 11, pp. 5879-5891, Nov. 2018.

[7] G. Oliveri, G. Gottardi, F. Robol, A. Polo, L. Poli, M. Salucci, M. Chuan, C. Massagrande, P. Vinetti, M. Mattivi, R. Lombardi, and A. Massa, "Co-design of unconventional array architectures and antenna elements for 5G base station," IEEE Trans. Antennas Propag., vol. 65, no. 12, pp. 6752-6767, Dec. 2017.

[8] N. Anselmi, P. Rocca, M. Salucci, and A. Massa, "Irregular phased array tiling by means of analytic schemata-driven optimization," IEEE Trans. Antennas Propag., vol. 65, no. 9, pp. 4495-4510, September 2017.

[9] N. Anselmi, P. Rocca, M. Salucci, and A. Massa, "Optimization of excitation tolerances for robust beamforming in linear arrays" IET Microwaves, Antennas & Propagation, vol. 10, no. 2, pp. 208-214, 2016.

[10] P. Rocca, R. J. Mailloux, and G. Toso, "GA-Based optimization of irregular sub-array layouts for wideband phased arrays desig," IEEE Antennas and Wireless Propag. Lett., vol. 14, pp. 131-134, 2015.

[11] P. Rocca, M. Donelli, G. Oliveri, F. Viani, and A. Massa, "Reconfigurable sum-difference pattern by means of parasitic elements for forward-looking monopulse radar," IET Radar, Sonar & Navigation, vol 7, no. 7, pp. 747-754, 2013.

[12] M. Salucci, G. Oliveri, M. A. Hannan, and A. Massa, âSystem-by-design paradigm-based synthesis of complex systems: The case of spline-contoured 3D radomes,â IEEE Antennas and Propagation Magazine â Special Issue on âArtificial Intelligence in Electromagnetics,â, vol. 64, no. 1, pp. 72-83, Feb. 2022.

[13] G. Oliveri, A. Gelmini, A. Polo, N. Anselmi, and A. Massa, "System-by-design multi-scale synthesis of task-oriented reflectarrays," IEEE Trans. Antennas Propag., vol. 68, no. 4, pp. 2867-2882, Apr. 2020.

[14] N. Anselmi, L. Poli, P. Rocca, and A. Massa, "Design of simplified array layouts for preliminary experimental testing and validation of large AESAs," IEEE Trans. Antennas Propag., vol. 66, no. 12, pp. 6906-6920, Dec. 2018.

[15] M. Salucci, F. Robol, N. Anselmi, M. A. Hannan, P. Rocca, G. Oliveri, M. Donelli, and A. Massa, "S-Band spline-shaped aperture-stacked patch antenna for air traffic control applications," IEEE Tran. Antennas Propag., vol. 66, no. 8, pp. 4292-4297, Aug. 2018.

[16] M. Salucci, L. Poli, A. F. Morabito, and P. Rocca, "Adaptive nulling through subarray switching in planar antenna arrays," Journal of Electromagnetic Waves and Applications, vol. 30, no. 3, pp. 404-414, February 2016

[17] T. Moriyama, L. Poli, and P. Rocca, "Adaptive nulling in thinned planar arrays through genetic algorithms" IEICE Electronics Express, vol. 11, no. 21, pp. 1-9, Sep. 2014.

[18] L. Poli, P. Rocca, M. Salucci, and A. Massa, "Reconfigurable thinning for the adaptive control of linear arrays," IEEE Trans. Antennas Propag., vol. 61, no. 10, pp. 5068-5077, Oct. 2013.

[19] P. Rocca, L. Poli, G. Oliveri, and A. Massa, "Adaptive nulling in time-varying scenarios through time-modulated linear arrays," IEEE Antennas Wireless Propag. Lett., vol. 11, pp. 101-104, 2012.

[20] L. Poli, D. Masotti, M. A. Hannan, A. Costanzo, and P. Rocca, "Codesign of switching sequence and diode parameters for multiple pattern optimization in time-modulated arrays," IEEE Antennas Wireless Propag. Lett. â Special Issue on âSpace-Time Modulated Antennas and Materialsâ, vol. 19, no. 11, pp. 1852-1856, Nov. 2020.

[21] P. Rocca, F. Yang, L. Poli, and S. Yang, "Time-modulated array antennas - Theory, techniques, and applications" Journal of Electromagnetic Waves and Applications, vol. 33, no. 12, pp. 1503-1531, Jun. 2019.

[22] L. Poli, P. Rocca, G. Oliveri, M. Chuan, C. Mazzucco, S. Verzura, R. Lombardi, and A. Massa, "Advanced pulse sequence design in time-modulated arrays for cognitive radio," IEEE Antennas Wireless Propagat. Lett., vol. 17, no. 5, pp. 898-902, May 2018.

[23] P. Rocca, G. Oliveri, R. J. Mailloux, and A. Massa, "Unconventional phased array architectures and design Methodologies - A review," Proceedings of the IEEE - Special Issue on 'Phased Array Technologies', Invited Paper, vol. 104, no. 3, pp. 544-560, March 2016.

[24] L. Poli, P. Rocca, G. Oliveri, and A. Massa, "Failure correction in time-modulated linear arrays," IET Radar, Sonar & Navigation, vol. 8, no. 3, pp. 195-201, 2014.

[25] L. Poli, T. Moriyama, and P. Rocca, "Pulse splitting for harmonic beamforming in time-modulated linear arrays," International Journal of Antennas and Propagation, vol. 2014, pp. 1-9, 2014.

[26] P. Rocca, Q. Zhu, E.T. Bekele, S. Yang, A. Massa, "4D arrays as enabling technology for cognitive radio systems" IEEE Trans. Antennas Propag., vol. 62, no. 3. pp. 1102-1116, Mar. 2014.

[27] E. T. Bekele, L. Poli, M. D'Urso, P. Rocca, and A. Massa, "Pulse-shaping strategy for time modulated arrays - Analysis and design," IEEE Trans. Antennas Propag., vol. 61, no. 7, pp. 3525-3537, July 2013.

[28] P. Rocca, M. D'Urso, and L. Poli, An iterative approach for the synthesis of optimized sparse time-modulated linear arrays," Progress In Electromagnetics Research B, vol. 55, pp. 365-382, 2013.

[29] P. Rocca, L. Poli, G. Oliveri, and A. Massa, "Adaptive nulling in time-varying scenarios through time-modulated linear arrays," IEEE Antennas Wireless Propag. Lett., vol. 11, pp. 101-104, 2012.

[30] P. Rocca, L. Poli, and A. Massa, "Instantaneous directivity optimization in time-modulated array receivers," IET Microwaves, Antennas & Propagation, vol. 6, no. 14, pp. 1590-1597, Nov. 2012.

[31] P. Rocca, L. Poli, L. Manica, and A. Massa, "Synthesis of monopulse time-modulated planar arrays with controlled sideband radiation," IET Radar, Sonar & Navigation, vol. 6, no. 6, pp. 432-442, 2012.

[32] L. Poli, P. Rocca, and A. Massa, "Sideband radiation reduction exploiting pattern multiplication in directive time-modulated linear arrays," IET Microwaves, Antennas & Propagation, vol. 6, no. 2, pp. 214-222, 2012.

[33] P. Rocca, L. Poli, A. Polo, and A. Massa, "Optimal excitation matching strategy for sub-arrayed phased linear arrays generating arbitrary shaped beams," IEEE Trans. Antennas Propag., vol. 68, no. 6, pp. 4638-4647, Jun. 2020.

[34] G. Oliveri, G. Gottardi and A. Massa, "A new meta-paradigm for the synthesis of antenna arrays for future wireless communications," IEEE Trans. Antennas Propag., vol. 67, no. 6, pp. 3774-3788, Jun. 2019.

[35] P. Rocca, M. H. Hannan, L. Poli, N. Anselmi, and A. Massa, "Optimal phase-matching strategy for beam scanning of sub-arrayed phased arrays," IEEE Trans. Antennas and Propag., vol. 67, no. 2, pp. 951-959, Feb. 2019.

[36] N. Anselmi, P. Rocca, M. Salucci, and A. Massa, "Contiguous phase-clustering in multibeam-on-receive scanning arrays" IEEE Trans. Antennas Propag., vol. 66, no. 11, pp. 5879-5891, Nov. 2018.

[37] L. Poli, G. Oliveri, P. Rocca, M. Salucci, and A. Massa, "Long-Distance WPT Unconventional Arrays Synthesis" Journal of Electromagnetic Waves and Applications, vol. 31, no. 14, pp. 1399-1420, Jul. 2017.

[38] G. Gottardi, L. Poli, P. Rocca, A. Montanari, A. Aprile, and A. Massa, "Optimal Monopulse Beamforming for Side-Looking Airborne Radars," IEEE Antennas Wireless Propag. Lett., vol. 16, pp. 1221-1224, 2017.

[39] G. Oliveri, M. Salucci, and A. Massa, "Synthesis of modular contiguously clustered linear arrays through a sparseness-regularized solver," IEEE Trans. Antennas Propag., vol. 64, no. 10, pp. 4277-4287, Oct. 2016.

[40] P. Rocca, G. Oliveri, R. J. Mailloux, and A. Massa, "Unconventional phased array architectures and design Methodologies - A review" Proceedings of the IEEE = Special Issue on 'Phased Array Technologies', Invited Paper, vol. 104, no. 3, pp. 544-560, March 2016.

[41] P. Rocca, M. D'Urso, and L. Poli,"Advanced strategy for large antenna array design with subarray-only amplitude and phase contr," IEEE Antennas and Wireless Propag. Lett., vol. 13, pp. 91-94, 2014.